Effects of different factors on ^{235}U mass estimation for natural and depleted uranium samples with different containers using the Active-Well Neutron Coincidence Counter

M.H. Hazzaa[1] , W.I. Zidan [1], N.M. Ibrahiem [1], A.G. Mostafa [2]* and M.Y. Hassaan [2]

[1.] Egyptian Nuclear and Radiological Regulatory Authority (ENRRA), Department of Nuclear Safeguards and Physical Protection, 3 Ahmad El-Zomor Str., El-Zohoor Dist., Nasr City, P.O. Code 11762, Cairo, Egypt
[2.] ME Lab., Phys. Dept., Faculty of Science, Al-Azhar Univ., Nasr City, Cairo, Egypt
*drahmedgamal@yahoo.com

Abstract: Effects of different factors on ^{235}U mass estimation in natural and depleted uranium samples, are carried out by measuring the coincidence count rates due to uranium isotopes using the Active-Well Neutron Coincidence Counter (AWCC) with and without containers. NM samples of different shapes, configurations and various chemical compositions, were contained, by aluminum (Al), lead (Pb) or polyethylene (PE) with different thicknesses (0.5, 1, 1.5 or 2 cm) for the estimation of ^{235}U mass. A semi-empirical calibration curves relate ^{235}U mass content in each modeled setup configuration with the corresponding measured coincidence count rate, were constructed with and without containers. The estimated ^{235}U mass content was found to be reduced by factors, where these factors were calculated for each sample type and for the rectangular and cylindrical shapes as well as for all configuration.
[Hazzaa MH, Zidan WI, Ibrahiem NM, Mostafa AG and Hassaan MY. **Effects of different factors on ^{235}U mass estimation for natural and depleted uranium samples with different containers using the Active-Well Neutron Coincidence Counter.** *Nat Sci* 2015;13(11):152-161]. (ISSN: 1545-0740). http://www.sciencepub.net/nature. 21. doi:10.7537/marsnsj131115.21.

Keywords: Nuclear safeguards; Uranium mass content; Monte Carlo; AWCC; Al; Pb; polyethylene

1. Introduction

It is known that the basic measure of a state system of accounting for and control (SSAC) of all nuclear material is NM accountancy [1, 2]. NMs, mainly uranium and plutonium, can be presented in different physical, chemical and geometrical forms. They may exist as metals or compounds, in solid, liquid or gaseous states. Uranium appears the most important NM and its mass has to be verified during inspection activities. The SSAC must include a measuring system which can be applied for all types of NM [3- 5].

The Active-Well Neutron Coincidence Counter (AWCC) is a coincidence neutrons counting system. It was designed as non-destructively assay (NDA) ^{235}U-bearing materials [6].

Many articles have been published in which the AWCC was tested and used in different applications. These articles demonstrated the applicability of AWCC for assaying uranium content in a wide variety of materials and generated calibration curves for different NM categories. Mykhaylov et al had obtained AWCC calibration curves for uranium metal and uranium dioxide with different enrichments up to 90 % [7]. David et al have made a comprehensive modeling study to evaluate the utility of multiple active neutron interrogation signatures for detecting shielded highly enriched uranium (HEU). The modeling effort focused on varying HEU masses from 1 kg up to 20 kg with different types of shields including cement, wood, polyethylene, aluminum, and steel at different depths of the HEU in the shields. Also they vary immediately the configuration of the shields surrounding the HEU including steel, lead, and cadmium. Neutron and gamma-ray signatures were the focus of the study [8]**.** Hee-Young Kang et al evaluate the neutron shielding effects of four materials, polyethylene, k-resin, paraffin and graphite by using a neutron source. The attenuation of the shielding materials were investigated for various thicknesses. The experiments were carried out with a ^{252}Cf source and three ^{3}He gas detectors as a long counter. The calculated results obtained from the Monte Carlo code were compared with the experimental measurements. They concluded that these materials can be used as neutron shields for spent fuel shipping casks, accelerators and neutron generators [9]. The effect of cosmic-ray shielding in passive neutron coincidence counting (PNCC) was studied by Alvarez and Wilkins. They present results from an experimental assessment and calculations of the effect of overhead shielding on the cosmic ray induced neutron events. Background data were taken with a pair of AWCC in different locations under different thicknesses and configuration of concrete to provide shielding from cosmic rays. Comparision are made with historical performance data as well as published work. These results will be useful when considering the location and shield of PNCC systems [10].

In most of the published work, it was noticed that, in order to obtain accurate quantitative

measurements, it is necessary to calibrate the instrument using physical standards representing the samples to be assayed. Generally, three different approaches might be used to address such issue; including semi-empirical calibration, cross calibration and Monte Carlo (MC) calculations. MC simulation codes could be used for mathematical calibration of the detectors to overcome the unavailability of NM standards [11-17].

In the present work a passive non-destructive assay (NDA) techniques (employing neutron or gamma ray spectrometry) has been used to study the effect of different factors affecting ^{235}U mass estimation.

A NM is contained inside aluminum (Al), lead (Pb) or polyethylene (PE), and the effect of containers on the estimation of ^{235}U mass by using the AWCC was proposed using semi-empirical calibration.

The facility at which this work was carried out is the Nuclear Chemical Building, Egyptian Atomic Energy Authority and the used NMs are subjected to the safeguards agreement between Egypt and the IAEA [MBA(ET-G), KMP(A)].

2. Experimental

2.1. System setup

The used AWCC system [Canberra, Model JCC-51] consists of a high-density polyethylene ring in which 42 ^{3}He thermal-neutron detectors [Reuter-Stokes model RS-P40820-103] are mounted in two concentric circles. The detectors are wired to give six groups of seven tubes for each. Each group is ganged through a single preamplifier/amplifier/discriminator board [JAB-01 Amptek]. The board output pulses are analyzed by the neutron analysis shift register [model JSR-141] together with the detector parameters shown in Table (1). The system consists of two $^{241}AmO_2$-Li neutron sources (7.6×10^4 n/s emission rate for each) to activate thermal fission in an assayed samples. Each source is kept in a stainless steel container. A tungsten shield is placed around each neutron source to reduce the gamma-ray emission [18-20].

Table 1. Detector parameters and timing characteristics used for this work [21]

Gate width	64 μsec
Predelay time	4.5 μsec
High voltage	1680 V
Die-away time	52.36 μsec

The AmLi neutron sources were positioned at 17.3 and 50.3 cm from the bottom of the detector (upper and lower locations respectively) to allow optimum sample interrogation. Al-Cd sleeves are removed from the detector cavity in order that, the counter operates in the active thermal mode. The measuring setup parameters for data acquisition are adjusted using Canberra NDA2000 Software [22].

2.2. Nuclear material measurements

Three rectangular pure metallic DU samples of 17.15 cm height and 3.2 cm length and 1.65 cm width, three cylinders of 18.2 cm length and 6 cm diameter containing powder natural $(NH_4)_2U_2O_7$ and other three cylinders of the same dimensions containing powder natural UF_4, have been used to measure the real coincidence neutrons count rate of ^{235}U with and without containers. These containers are aluminum, lead or polyethylene, where four cylinders of each container having 20 cm length and 6 cm inner diameter for each, differ only in their wall thickness (0.5, 1, 1.5 or 2 cm), and other four rectangulars of each container having 22.5 cm length and 5.2 cm wide and 4.6 cm height for each, the wall thickness of all containers are also (0.5, 1, 1.5 or 2 cm). Fig. (1) illustrates the different setup configurations of the AWCC for which the NM samples were measured inside the containers. For each setup configuration, the real fission coincidence neutron is calculated as the average of three measuring runs with and without containers.

The uncertainties for the coincidence counting rates ranged between 1.2% and 5% according to the number of measured cylinders and rectangular samples (from one to three cylinders and rectangular). The measuring times were 2400 sec.

3. Fission rate calculation

Fission rate of ^{235}U nuclei in NM samples measured in the AWCC depends on many parameters and factors [6, 23 & 24]. Monte Carlo modeling is an efficient and accurate method to calculate the fission rate using the multi-purpose MCNP-5 code via NM-detector geometry modeling, (as shown in Fig. [1]) [25].

Fission rate per unit volume was calculated using the track length estimation of cell flux (F4:N n) with the tally multiplier card (FMn C M R_1), where n is the cell number (which contains the NM), C is the atomic density of the material, M is the material number on material card and R_1 is the reaction number for total fission cross section, (R_1 = - 6).

Fission rate was calculated for each cylinder and rectangular shapes with different containers and thicknesses. This process was repeated for each NM sample in each setup configuration. Each calculational run was performed using 10^6 histories; the time of a run was about 20 minute on a 2.2 GHz Core2Duo processor. The relative standard deviation of the MCNP calculations did not exceed 2.5% for all runs.

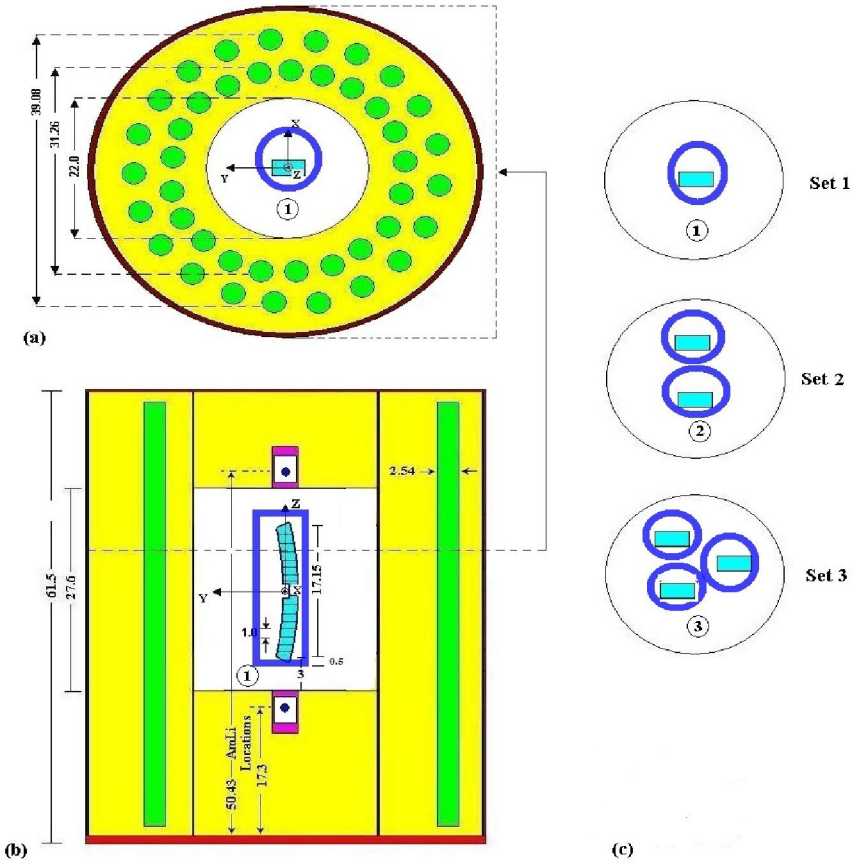

Figure 1. Geometrical model of the AWCC used for Monte Carlo calculations with different setup configurations of DU metal samples inside the cavity with containers. (a) Cross sectional view, (b) longitudinal view and (c) different setup configuration for the different sets

4. Results and Discussion

Fig.(2) shows the relation between the count rate and the wall thickness of different containers where they are found in agreement with Monte carol calculation for $(NH_4)_2U_2O_7$, UF_4 and DU metal matrices. That is the count rate decreased gradually with the increase of the wall thickness of the used containers.

^{235}U mass content with and without container in $(NH_4)_2U_2O_7$ and UF_4 as well as in DU metal matrices can be calculated for $(NH_4)_2U_2O_7$ and UF_4 from equation (4) and equation (5) for DU metal [21],

$$M_5 = \frac{Cr}{\pi r^2 S \sum_{i=1}^{n} \int_{3}^{21.2} f_{c5}(h).(A + Bh + Ch^2 + Dh^3).dh} \quad (4)$$

$$M_5 = \frac{R}{AS \sum_{i=1}^{n} \int_{3}^{20.15} f_{c5}(h).(Fr_0 + \sum_{j=1}^{3} \frac{A_{ij}}{w_{ij}\sqrt{\frac{\pi}{2}}} e^{-2\frac{(h-h_{cij})^2}{w_{ij}^2}}).dh} \quad (5)$$

Where $f_{c5}(h)$ is the coincidence efficiency of the detector and F_r is the fission rates per unit volume per NM sample,

$$F_r = F_5(h) = Fr_0 + \sum_{i=1}^{3} \frac{A_i}{w_i \sqrt{\frac{\pi}{2}}} e^{-2\frac{(h-hc_i)^2}{w_i^2}},$$

$$F_r = F_5(h) = A + Bh + Ch^2 + Dh^3$$

The results of the real coincidence count rate with container as a function of ^{235}U mass content corresponding to each setup configuration were fitted by second order polynomial applied to construct the calibration curve, which leads to calculate the ^{235}U mass for $(NH_4)_2U_2O_7$, UF_4 and DU metal matrices.

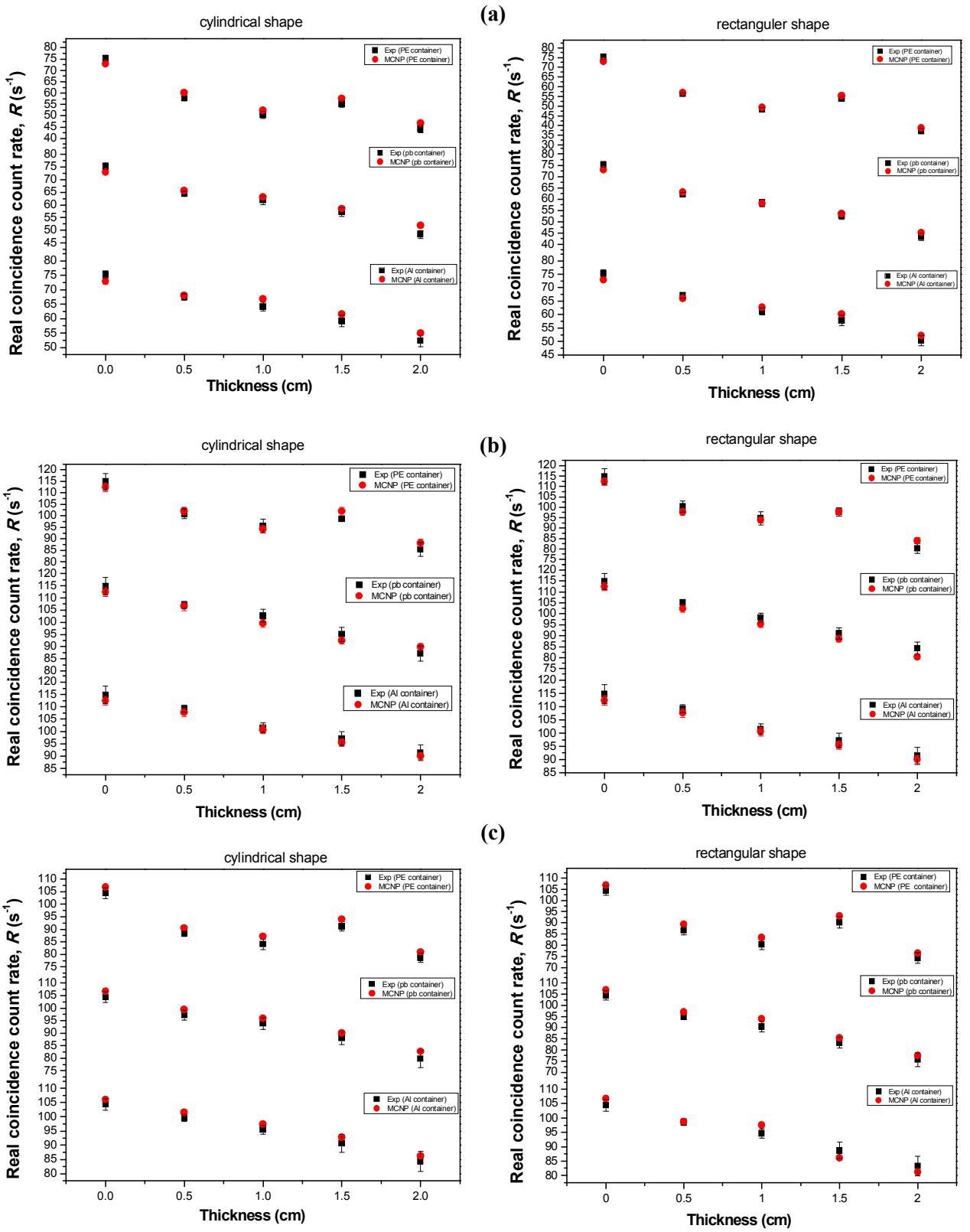

Figure 2. The variation of the real coincidence count rate with the thickness of different containers and shapes. (a) $(NH_4)_2U_2O_7$ matrix, (b) (UF_4) matrix and (c) DU metal

Fig. (3) shows the variation of the real coincidence count rate with ^{235}U mass content corresponding to each setup configuration and for different containers. For $(NH_4)_2U_2O_7$ matrix with cylindrical shape without container the real count rate is 75.3 c/s and the ^{235}U mass content is 3.311 g for set (1), but it is 122.2 c/s and 6.248 g for set (2) and it is 178.3 c/s and 9.309 g for set (3). For Al container (0.5 cm thickness) the real count rate decreased and the ^{235}U mass content decreased to 2.789, 6.065 and 9.148 g for set (1, 2 and 3) respectively. For Pb container (0.5 cm thickness), the ^{235}U mass content decreased to 2.586, 5.945 and 8.867 g for sets (1, 2 and 3) respectively. For PE container (0.5 cm thickness), the ^{235}U mass content decreased to 2.113, 5.481 and 8.539 g for sets (1, 2 and 3) respectively. For rectangular shape there are small change for ^{235}U mass content as shown in Fig. (3a).

For (UF_4) matrix with cylindrical shape without container the real count rate is 114.8 c/s and the ^{235}U mass content is 5.207 g for set (1), but it is 228.3 c/s and 11.044 g for set (2) and it is 334.2 c/s and 16.891 g for set (3). For Al container (0.5 cm thickness) the real count rate decreased, then ^{235}U mass content decreased to 4.955, 10.879 and 16.669 g for sets (1, 2 and 3) respectively. For Pb container (0.5 cm thickness) ^{235}U mass content decreased to 4.832, 10.560 and 16.266 g for sets (1, 2 and 3) respectively. For PE container (0.5 cm thickness) ^{235}U mass content decreased to 4.518, 10.036 and 15.864 g for sets (1, 2 and 3) respectively. For rectangular shape there are small change for ^{235}U mass content as shown in Fig. (3b).

For DU metal with cylindrical shape without container the real count rate is 104.4 c/s and the ^{235}U mass content is 6.501 g for set (1), but it is 213.2 c/s and 12.841 g for set (2) while it is 283.4 c/s and 18.032 g for set (3). For Al container (0.5 cm thickness) the real count rate decreased, so the ^{235}U mass content is decreased to 6.168, 12.245 and 17.379 g for set (1, 2 and 3) respectively. For Pb container (0.5 cm thickness) ^{235}U mass content decreased to 5.714, 11.517 and 16.778 g for sets (1, 2 and 3) respectively. For PE container (0.5 cm thickness) the ^{235}U mass content is decreased to 5.139, 10.286 and 16.159 g for sets (1, 2 and 3) respectively. For rectangular shape there are small change for ^{235}U mass content as shown in Fig. (3c).

Fig. (4) shows the variation of ^{235}U mass content with different container shapes and thicknesses where it shows that ^{235}U mass contents for $(NH_4)_2U_2O_7$, UF_4 and DU metal matrices without container are 3.311, 5.207 and 6.501g respectively, and it shows gradual decrease with the increase of the wall thickness of the containers. It is shown that ^{235}U masses reduced by a factors of (0.842, 0.773, 0.672 or 0.527), (0.834, 0.713, 0.642 or 0.485) for aluminum containers of cylindrical and rectangular shapes, with thicknesses of (0.5, 1, 1.5 or 2 cm) respectively. But it reduced by factors of (0.781, 0.727, 0.632 or 0.444), (0.732, 0.653, 0.535 or 0.333) for lead container of thicknesses (0.5, 1, 1.5 or 2 cm) respectively, while for polyethylene container, it reduced by factors of (0.638, 0.485, 0.588 or 0.352), (0.608, 0.440, 0.561 or 0.201) of thicknesses (0.5, 1, 1.5 or 2 cm) respectively, for $(NH_4)_2U_2O_7$ matrix. All the obtained values are exhibited in Table (2, a & b) for cylindrical and rectangular shapes respectively.

(a)

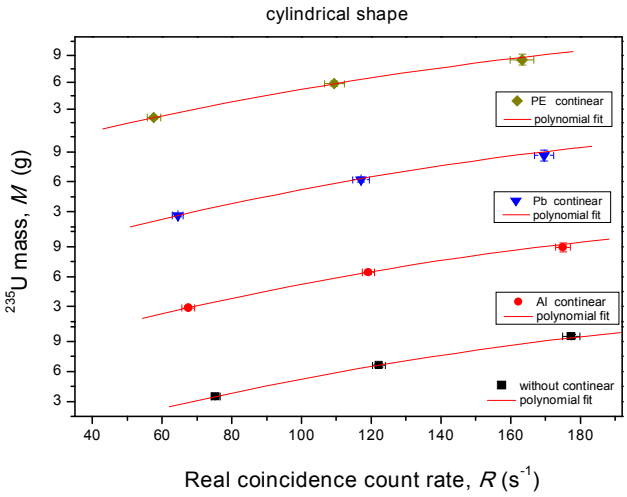

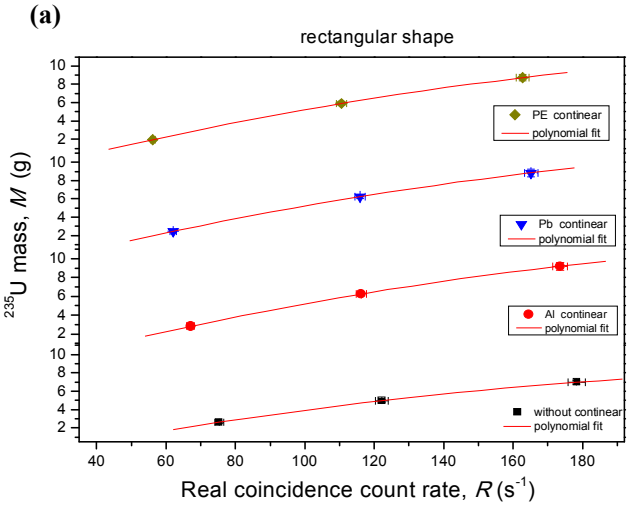

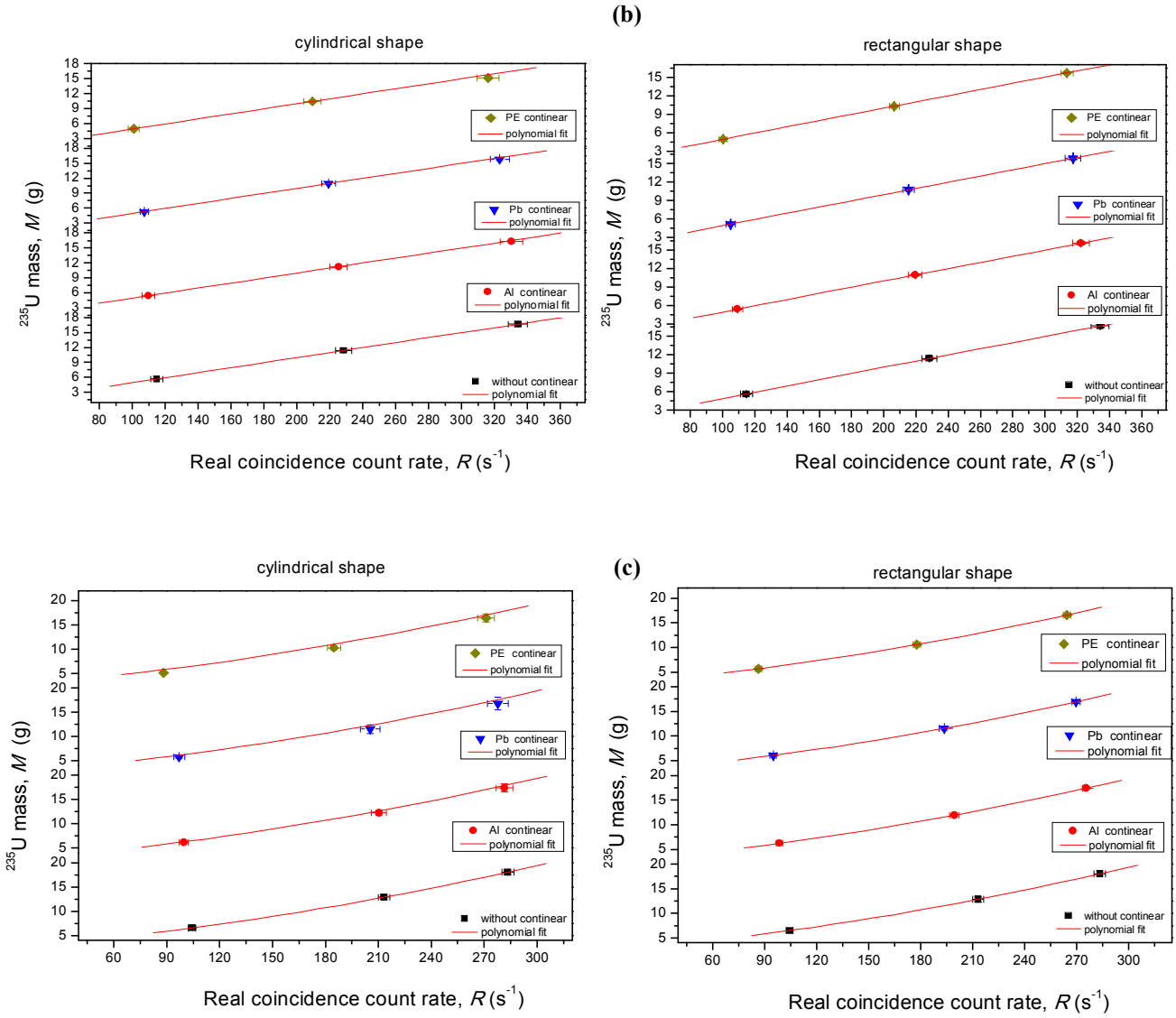

Figure 3. The variation of the real coincidence count rate with ^{235}U mass content for different containers and shapes. Solid line represents the second order polynomial fit of the estimated data (a) $(NH_4)_2U_2O_7$ matrix, (b) (UF_4) matrix and (c) DU metal

^{235}U masses reduced by factors of (0.952, 0.896, 0.842 or 0.771), (0.948, 0.874, 0.833 or 0.779) for aluminum containers of cylindrical and rectangular shapes, with thicknesses of (0.5, 1, 1.5 or 2 cm) respectively. But it reduced by factors (0.972, 0.886, 0.814 or 0.740), (0.908, 0.844, 0.777 or 0.712) for lead containers of thicknesses (0.5, 1, 1.5 or 2 cm) respectively, while for polyethylene container, it reduced by factors of (0.867, 0.818, 0.846 or 0.723), (0.862, 0.809, 0.838 or 0.675) of thicknesses (0.5, 1, 1.5 or 2 cm) respectively, for (UF_4) matrix.

It was found also that ^{235}U masses reduced by factors of (0.949, 0.888, 0.807 or 0.700), (0.894, 0.836, 0.747 or 0.632) for aluminum containers of cylindrical and rectangular shapes, with thicknesses of (0.5, 1, 1.5 or 2cm) respectively. But it reduced by factors of (0.884, 0.829, 0.712 or 0.637), (0.834, 0.805, 0.647 or 0.564) for lead container of thicknesses (0.5, 1, 1.5 or 2 cm) respectively, while for polyethylene container, it reduced by factors of (0.790, 0.744, 0.779 or 0.541), (0.777, 0.735, 0.758 or 0.482) of thicknesses (0.5, 1, 1.5 or 2 cm) respectively for DU metal. The increase of the real count rate and ^{235}U masses at thickness (1.5cm) polyethylene for all matrices raise the likelihood of generating fissions as shown as in Figs. (2&4).

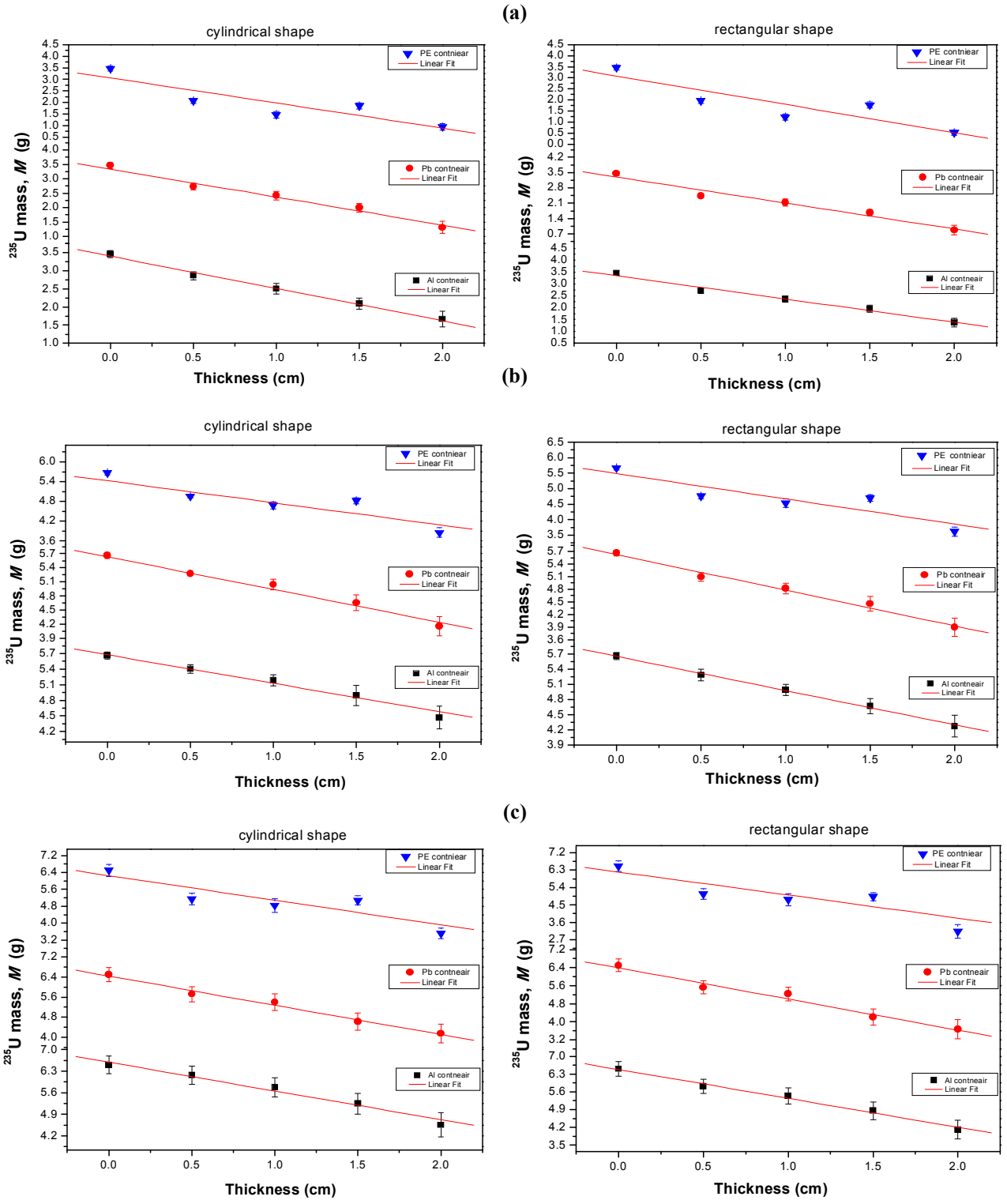

Figure 4. The variation of ^{235}U mass for the different containers and shapes with the thickness. Solid line represents the linear fit of the measured data (a) $(NH_4)_2U_2O_7$ matrix, (b) (UF_4) matrix and (c) DU metal

Table (2-a) ^{235}U mass content in each modeled setup configuration with different containers and wall thicknesses for cylindrical shape

With Containers / Thickness	$(NH_4)_2U_2O_7$ matrix cylindrical shape			(UF_4) matrix cylindrical shape			DU metal cylindrical shape		
	^{235}U Mass $(M_5,g)\pm\sigma_{M5}$ Al	^{235}U Mass $(M_5,g)\pm\sigma_{M5}$ Pb	^{235}U Mass $(M_5,g)\pm\sigma_{M5}$ PE	^{235}U Mass $(M_5,g)\pm\sigma_{M5}$ Al	^{235}U Mass $(M_5,g)\pm\sigma_{M5}$ Pb	^{235}U Mass $(M_5,g)\pm\sigma_{M5}$ PE	^{235}U Mass $(M_5,g)\pm\sigma_{M5}$ Al	^{235}U Mass $(M_5,g)\pm\sigma_{M5}$ Pb	^{235}U Mass $(M_5,g)\pm\sigma_{M5}$ PE
0.5 Cm	2.789±0.112	2.586±0.109	2.113±0.106	4.955±0.079	4.832±0.026	4.518±0.043	6.168±0.286	5.714±0.291	5.139±0.280
1 Cm	2.558±0.147	2.409±0.145	1.605±0.140	4.670±0.110	4.611±0.115	4.263±0.113	5.772±0.312	5.394±0.332	4.838±0.326
1.5 Cm	2.224±0.160	2.092±0.144	1.947±0.127	4.385±0.190	4.239±0.172	4.410±0.094	5.244±0.335	4.617±0.348	5.070±0.213
2 Cm	1.745±0.217	1.471±0.211	1.166±0.139	4.015±0.219	3.854±0.202	3.762±0.145	4.552±0.392	4.144±0.375	3.514±0.248
Set (2)	6.065±0.166	5.945±0.161	5.481±0.154	10.879±0.130	10.560±0.109	10.036±0.116	12.245±0.513	11.517±0.515	10.286±0.419
Set (3)	9.148±0.359	8.867±0.319	8.539±0.265	16.669±0.370	16.266±0.346	15.864±0.269	17.379±0.536	16.778±0.520	16.159±0.417
Transmission Factor (M_5/M_{5o})									
0.5 Cm	0.842	0.781	0.638	0.952	0.972	0.867	0.949	0884	0.790
1 Cm	0.773	0.727	0.485	0.896	0.886	0.818	0.888	0.829	0.744
1.5 Cm	0.672	0.632	0.588	0.842	0.814	0.846	0.807	0.712	0.779
2 Cm	0.527	0.444	0.352	0.771	0.740	0.723	0.700	0.637	0.541
Set (2)	0.971	0.951	0.877	0.985	0.956	0.908	0.954	0.897	0.801
Set (3)	0.983	0.953	0.917	0.986	0.962	0.939	0.964	0.930	0.896
Without Containers									
Set (1)	3.311±0.084			5.207±0.136			6.501±0.285		
Set (2)	6.248±0.189			11.044±0.295			12.841±0.503		
Set (3)	9.309±0.388			16.891±0.364			18.032±0.584		

Table (2-b) ^{235}U mass content in each modeled setup configuration with different containers and wall thicknesses for rectangular shape

With Containers / Thickness	$(NH_4)_2U_2O_7$ matrix rectangular shape			(UF4) matrix rectangular shape			DU metal rectangular shape		
	^{235}U Mass (M_5,g)±σ_{M5} Al	^{235}U Mass (M_5,g)±σ_{M5} Pb	^{235}U Mass (M_5,g)±σ_{M5} PE	^{235}U Mass (M_5,g)±σ_{M5} Al	^{235}U Mass (M_5,g)±σ_{M5} Pb	^{235}U Mass (M_5,g)±σ_{M5} PE	^{235}U Mass (M_5,g)±σ_{M5} Al	^{235}U Mass (M_5,g)±σ_{M5} Pb	^{235}U Mass (M_5,g)±σ_{M5} PE
0.5 Cm	2.762±0.109	2.422±0.107	2.016±0.115	4.935±0.111	4.728±0.101	4.494±0.080	5.816±0.287	5.423±0.291	5.056±0.276
1 Cm	2.360±0.122	2.162±0.163	1.457±0.138	4.935±0.112	4.395±0.125	4.214±0.137	5.432±0.320	5.235±0.306	4.776±0.315
1.5 Cm	2.127±0.147	1.773±0.134	1.856±0.136	4.341±0.151	4.044±0.176	4.366±0.106	4.857±0.345	4.207±0.358	4.926±0.213
2 Cm	1.604±0.179	1.103±0.218	0.665±0.114	4.059±0.211	3.709±0.217	3.516±0.151	4.111±0.368	3.669±0.419	3.136±0.351
Set (2)	5.892±0.171	5.874±0.179	5.547±0.163	10.576±0.092	10.358±0.088	9.888±0.079	11.821±0.242	11.145±0.312	9.950±0.175
Set (3)	9.072±0.324	8.639±0.343	8.513±0.258	16.215±0.311	15.933±0.312	15.718±0.255	17.004±0.302	16.342±0.520	15.741±0.298
Transmission Factor (M_5/M_{5o})									
0.5 Cm	0.834	0.732	0.608	0.948	0.908	0.862	0.894	0.834	0.777
1 Cm	0.713	0.653	0.440	0.874	0.844	0.809	0.836	0.805	0.735
1.5 Cm	0.642	0.535	0.561	0.833	0.777	0.838	0.747	0.647	0.758
2 Cm	0.485	0.333	0.201	0.779	0.712	0.675	0.632	0.564	0.482
Set (2)	0.943	0.940	0.887	0.957	0.937	0.895	0.921	0.867	0.775
Set (3)	0.974	0.928	0.914	0.959	0.943	0.930	0.943	0.906	0.873
Without Containers									
Set (1)	3.311±0.084			5.207±0.136			6.501±0.285		
Set (2)	6.248±0.189			11.044±0.295			12.841±0.503		
Set (3)	9.309±0.388			16.891±0.364			18.032±0.584		

5. Conclusion

A semi-empirical calibration curve relates ^{235}U mass content in each modeled setup configuration with its corresponding measured coincidence count rate, was constructed with and without containers. From these curves, ^{235}U mass contents can be deduced, for different containers (Al, Pb or PE). According to these studies, it can be concluded that ^{235}U mass contents decreased with the gradual increase of the wall thickness containers. Factors of correction for each container and its thickness were obtained which can be used to calculate the correct ^{235}U masses in any NMs. The count rates are found in complete agreement with the measured values within

the limits of error. It is found also that, by using MCNP code, the correction factors due to the using of different containers can be also deduced.

Corresponding Author:
Prof. Dr. A. G. Mostafa
ME Lab., Phys. Dept.
Faculty of Science,
Al-Azhar Univ., Nasr City, Cairo, Egypt
E-mail: *drahmedgamal@yahoo.com

References

1. The structure and content of agreements between the agency and states required in connection with the nonproliferation treaty of nuclear weapons, IAEA Doc. INFCIRC/153 (Corr.), Vienna, Austria (1972).
2. Guidelines for states' systems of accounting for and control of nuclear materials, IAEA/SG/INF/2, IAEA, Vienna, Austria (1980).
3. Safeguards techniques and equipment, International nuclear verification series No.1, IAEA, Vienna, Austria (1997).
4. T. D. Reilly, N. Ensslin, H. A. Smith and Jr. S. Kreiner, "Passive nondestructive assay of nuclear materials", Los Alamos National Laboratory, United States Nuclear Regulatory Commission, NUREG/CR-5550, (LA-UR-90-732) (1991).
5. W. El-Gammal, M. El-Nagdy, M. Rizk, S. Shawky and M. A. Samei, Nucl. Instr. and Meth. A, 553 (2005) 627.
6. H. O. Menlove, "Description and operation manual for the active well coincidence counter", Los Alamos National Laboratory, (LA-7823-M) (1979).
7. V. Mykhaylov, M. Odeychuk, V. Tovkanetz, V. Lapshyn, K. Thompson and J. Leicman, Symposium on international safeguards, (IAEA-SM-367/4/04/p), Vienna, Austria, 29 Oct - 2 Nov (2001).
8. David L. Chichester, Scott J. Thompson, Scott M. Watson, James T. Johnson and Edward H. Seabury, IEEE Nuclear Science Symposi, (INL/CON-12-25806), USA (2012).
9. Hee-Young Kang, Chang-Jae Park, Ki-Seog Seo and Ji-Sup Yoon, J. Korean Physical Society, 52 (2008) 6.
10. E. Alvarez, and C. G. Wilkins, Tucson Conference, A Z February 26-March 2 (2006).
11. G. Fehrenbacher, R. Meckbach and P. Jacob, Nucl. Instr. and Meth. A, 383 (1996) 454.
12. J. Denas, A. Martinavarro and V. Rius, Nucl. Instr. and Meth. A, 450 (2000) 88.
13. M. Korun, A. Likar and T. Vidmar, Nucl. Instr. and Meth. A, 390 (1997) 203.
14. S. Ashrfi, A. Likar and T. Vidmar, Nucl. Instr. and Meth. A, 438 (1999) 421.
15. M. A. Ludington and R. G. Helmer, Nucl. Instr. and Meth. A, 446 (2000) 506.
16. K. Debertin and B. Grosswendt, Nucl. Instr. and Meth. A, 203 (1982) 343.
17. T. Vidmar, M. Korun, A. Likar and R. Martincic, Nucl. Instr. and Meth. A, 470 (2001) 533.
18. CANBERRA, Active well neutron coincidence counter, Model JCC-51, User's manual, USA (1998).
19. CANBERRA, Neutron coincidence counter checklist, ^{3}He tube data sheets, USA (1998).
20. CANBERRA, Neutron analysis shift register, Model JSR-14, User's manual, USA (1997).
21. W. El-Gammal, W. I. Zidan and E. Elhakim, Nucl. Instr. And Meth. (A), 565 (2006) 731.
22. CANBERRA, NDA 2000 Non-Destructive Assay Software, USA (2006).
23. CANBERRA, Active well neutron coincidence counter, Model JCC-51, User's manual, USA (1998).
24. CANBERRA, Neutron coincidence counter checklist, 3He tube data sheets, USA (1998).
25. Jeremy E. Sweezy (MCNP Team Leader.), MCNPTM—A general Monte Carlo N-particle transport code (Version 5), (LA-12625-M), April 24 (2003) (Revised 10/3/05).

11/25/2015